Biochemical and Biophysical Research Communications 449 (2014) 196–201

Contents lists available at ScienceDirect

Biochemical and Biophysical Research Communications

journal homepage: www.elsevier.com/locate/ybbrc

Time-resolved FRET reveals the structural mechanism of SERCA–PLB regulation

Xiaoqiong Dong [a], David D. Thomas [b,*]

[a] Department of Biomedical Engineering, University of Minnesota, Minneapolis, MN 55455, USA
[b] Department of Biochemistry, Molecular Biology and Biophysics, University of Minnesota, Minneapolis, MN 55455, USA

ARTICLE INFO

Article history:
Received 15 April 2014
Available online 9 May 2014

Keywords:
Phospholamban
SERCA
Phosphorylation
FRET

ABSTRACT

We have used time-resolved fluorescence resonance energy transfer (TR-FRET) to characterize the interaction between phospholamban (PLB) and the sarcoplasmic reticulum (SR) Ca-ATPase (SERCA) under conditions that relieve SERCA inhibition. Unphosphorylated PLB inhibits SERCA in cardiac SR, but inhibition is relieved by either micromolar Ca^{2+} or PLB phosphorylation. In both cases, it has been proposed that inhibition is relieved by dissociation of the complex. To test this hypothesis, we attached fluorophores to the cytoplasmic domains of SERCA and PLB, and reconstituted them functionally in lipid bilayers. TR-FRET, which permitted simultaneous measurement of SERCA–PLB binding and structure, was measured as a function of PLB phosphorylation and [Ca^{2+}]. In all cases, two structural states of the SERCA–PLB complex were resolved, probably corresponding to the previously described *T* and *R* structural states of the PLB cytoplasmic domain. Phosphorylation of PLB at S16 completely relieved inhibition, partially dissociated the SERCA–PLB complex, and shifted the T/R equilibrium within the bound complex toward the *R* state. Since the PLB concentration in cardiac SR is at least 10 times that in our FRET measurements, we calculate that most of SERCA contains bound phosphorylated PLB in cardiac SR, even after complete phosphorylation. 4 μM Ca^{2+} completely relieved inhibition but did not induce a detectable change in SERCA–PLB binding or cytoplasmic domain structure, suggesting a mechanism involving structural changes in SERCA's transmembrane domain. We conclude that Ca^{2+} and PLB phosphorylation relieve SERCA–PLB inhibition by distinct mechanisms, but both are achieved primarily by structural changes within the SERCA–PLB complex, not by dissociation of that complex.

1. Introduction

A hallmark of heart failure is dysregulation of intracellular Ca^{2+} handling [1], primarily caused by inadequate removal of Ca^{2+} from the cytosol by the sarco(endo)plasmic reticulum Ca^{2+}-ATPase (SERCA) [2], which actively sequesters Ca^{2+} back into the sarcoplasmic reticulum (SR) at a ratio of 2 Ca^{2+} per ATP hydrolyzed [3]. In the heart, SERCA is regulated by phospholamban (PLB), a single-pass integral membrane protein. Unphosphorylated PLB inhibits SERCA by decreasing its apparent Ca^{2+} affinity [4]. Under physiological conditions, this inhibition is relieved by either micromolar Ca^{2+} or by phosphorylation of PLB, primarily by protein kinase A (PKA) at S16 [5]. Recent gene therapies targeting increased SERCA activity show promise for alleviation of heart failure [6]. Ablation of PLB or introduction of phosphomimetic mutant S16E-PLB suppress progression of heart failure in animal models [7–9]. Overexpression of SERCA2a, the cardiac isoform, has successfully completed Phase IIa clinical trials [10]. These studies validate the SERCA–PLB complex as a potent therapeutic target for heart failure. However, rational design of improved therapies is hampered by uncertainty regarding the mechanism by which PLB regulates SERCA.

Two structural mechanisms for relief of SERCA inhibition have been proposed. The dissociation model hypothesizes that PLB dissociates from SERCA to relieve inhibition. This model is supported by crosslinking and co-immunoprecipitation studies that found decreased physical interaction between SERCA and

Abbreviations: IAF, 5-iodoacetamidofluorescein; DOPC, 1,2-dioleoyl-*sn*-glycero-3-phosphocholine; DOPE, 1,2-dioleoyl-*sn*-glycero-3-phosphoethanolamine; EGTA, ethylene glycol-bis-(2-aminoethylether)-N,N,N′,N′-tetraacetic acid; ESI-MS, electrospray ionization mass spectroscopy; FRET, fluorescence resonance energy transfer; TR-FRET, time-resolved FRET; MOPS, 3-(*N*-morpholino)propanesulfonic acid; pCa, $-\log_{10}[Ca^{2+}]$; pK_{Ca}, $-\log(K_{Ca})$, calcium concentration at half-maximal ATPase activity; PLB, phospholamban; SERCA, sarco(endo)plasmic reticulum Ca^{2+}-ATPase; SR, sarcoplasmic reticulum; OG, octyl β-D-glucopyranoside; PKA, protein kinase A.

* Corresponding author. Fax: +1 (612) 624 0632.
E-mail address: ddt@umn.edu (D.D. Thomas).

http://dx.doi.org/10.1016/j.bbrc.2014.04.166
0006-291X/

PLB at either micromolar Ca^{2+} or after phosphorylation at S16 by PKA [11–16]. However, recent spectroscopic studies support the subunit model, in which inhibition of SERCA is relieved by structural rearrangements within the SERCA–PLB complex, not by dissociation. Electron paramagnetic resonance (EPR) and fluorescence resonance energy transfer (FRET) studies showed that PLB remains bound to SERCA when the pump is activated [17–20]. EPR and NMR studies showed that the cytoplasmic domain of PLB exists in equilibrium between a *T* state that is ordered and an *R* state that is dynamically disordered [21–23]. Phosphorylation shifts the equilibrium toward the *R* state and relieves inhibition [24]. FRET studies showed that variation of lipid headgroup charge shows a strong correlation between the population of the *R* state and SERCA–PLB activation, without dissociation, further validating the subunit model [25]. That study showed the power of time-resolved (TR) FRET to distinguish between changes in structure and association. In the present study, we have used TR-FRET, using fluorophore-labeled SERCA and PLB reconstituted in lipid bilayers, to resolve the effects of both micromolar Ca^{2+} and PLB phosphorylation on the structure and stability of the SERCA–PLB complex. These results provide definitive insights into the molecular mechanisms underlying relief of inhibition in cardiac SR.

2. Materials and methods

2.1. SERCA purification and labeling

Crude SR vesicles were prepared from the fast-twitch skeletal muscle of New Zealand white rabbits [26]. SERCA was further purified from crude SR vesicles using reactive-red chromatography [27]. For FRET studies, purified SERCA was labeled with 5-iodoacetamidofluorescein (IAF) (Invitrogen, CA) specifically and completely at C674 [28].

2.2. Expression, purification, phosphorylation and labeling of PLB

Native PLB equilibrates between monomers and homopentamers [29]. To simplify the analysis and focus on the SERCA–PLB interaction, a monomeric mutant of PLB was used, with the three cysteine residues (C36, C41 and C46) in the transmembrane domain mutated to alanine, phenylalanine, and alanine, respectively [30]. Site-directed mutagenesis was performed to mutate Y6 to C for thiol-reactive fluorophore attachment. This site was chosen because Y6 is not involved in the interaction with SERCA [31]. Recombinant PLB was expressed in *Escherichia coli* and purified as previously published [32]. For site-directed fluorophore labeling, lyophilized PLB powder was dissolved at a concentration of 0.2 mM in 20 mM MOPS, 1% octyl β-D-glucopyranoside (OG), pH 7.0. Alexa Fluor®350 C_5 maleimide (Invitrogen, CA) freshly dissolved in DMSO was then added at 10-fold molar excess. The reaction was allowed to proceed at room temperature for 1 h, and the labeled PLB was purified by reversed-phase HPLC. For phosphorylation studies, labeled PLB was phosphorylated as described previously [29] and purified by reversed-phase HPLC. Complete labeling and phosphorylation of PLB was confirmed by ESI-MS. The concentration of PLB was measured by the BCA assay.

2.3. Co-reconstitution of SERCA and PLB

SERCA and PLB were co-reconstituted into lipid vesicles using 4:1 1,2-dioleoyl-*sn*-glycero-3-phosphocholine (DOPC)/1,2-dioleoyl-*sn*-glycero-3-phosphoethanolamine (DOPE) (mol/mol) to yield unilamellar vesicles [33]. Ca^{2+}-ATPase activity and FRET measurements were performed immediately after co-reconstitution. The final buffer composition of FRET samples was 50 mM MOPS, 100 mM KCl, 5 mM $MgCl_2$, 1 mM EGTA, pH 7.0, with varying concentrations of $CaCl_2$ to yield the desired free Ca^{2+} concentration (pCa 8.0, 6.4, or 5.4).

2.4. Ca^{2+}-ATPase functional measurements

To ensure that labeled SERCA and PLB remain functional, we measured the ATPase activity of co-reconstituted samples at 25 °C, using an NADH-linked enzyme-coupled assay [33,34]. The Ca^{2+}-dependent rate of ATP consumption was fitted to the Hill equation,

$$V = V_{max}/[1 + 10^{-n(pK_{Ca} - pCa)}], \quad (1)$$

where $pCa = -\log_{10}[Ca^{2+}]$, V_{max} is the limiting activity at saturating calcium, pK_{Ca} is the pCa value where $V = 0.5V_{max}$, and n is the Hill coefficient. The inhibition of SERCA by PLB is shown as ΔpK_{Ca}, the shift of pK_{Ca} upon addition of PLB.

2.5. Time-resolved fluorescence resonance energy transfer (TR-FRET) measurements

SERCA and PLB were labeled with fluorophores at the sites shown in Fig. 1A. PLB was labeled with Alexa Fluor 350 maleimide (donor) at Y6C, and SERCA was labeled with IAF (acceptor) at C674. The quantum yield of bound Alexa Fluor 350 maleimide was measured in 20 mM MOPS, 1% OG, pH 7.0, using quinine sulfate dehydrate (AnaSpec, CA) as the standard, yielding a quantum yield of 0.48 for PLB, 0.80 for phosphorylated PLB (pPLB). The corresponding R_0 values [35] are calculated to be 4.6 nm and 5.0 nm, respectively. The time-resolved fluorescence decay of co-reconstituted samples was measured by time-correlated single-photon counting (Becker-Hickl, Berlin, Germany), following excitation at 385 nm using a subnanosecond pulsed diode laser (PicoQuant, Berlin, Germany), filtering the emitted light using a 440/40 filter (Semrock, NY), and detection with a PMH-100 photomultiplier (Becker-Hickl). The instrument response function (IRF, Fig. 1B) was recorded from water. TR-FRET data was analyzed as previously published [25]. The observed donor-only waveform (Fig. 1B) was fitted by a simulation $F_{Dsim}(t)$, consisting of a multi-exponential decay $F_D(t)$ convoluted with the IRF.

$$F_D(t) = \sum_{i=1}^{n} A_i \exp(t/\tau_{Di}) \quad (2)$$

$$F_{Dsim}(t) = \int_{-\infty}^{+\infty} IRF(t - t')F_D(t')dt'$$

where τ_{Di} is the fluorescence lifetime of the ith component. In this study, two exponentials were sufficient to fit the donor-only waveform (Fig. S1). The waveform of the samples containing donor and acceptor (Fig. 1B), was fitted by $F_{D+A,sim}(t)$:

$$F_{D+A}(t) = (1 - x_{DA})F_D(t) + x_{DA}\sum_{i=1}^{m} F_{DA,j}(t)$$

$$F_{D+A,sim}(t) = \int_{-\infty}^{\infty} IRF(t - t')F_{D+A}(t')dt', \quad (3)$$

where x_{DA} is the mole fraction of donor-labeled PLB that is bound to acceptor-labeled SERCA, and $F_{DA,j}(t)$ is the fluorescence waveform of the jth donor–acceptor complex. We found that $m = 2$ was sufficient (Fig. S3).

$$F_{DA}(t) = \int_{-\infty}^{+\infty} \rho(R)\sum_{i=1}^{n} A_i \exp\{(-t/\tau_{Di})[1 + (R_{oi}/R)^6]\}dR \quad (4)$$

where R_{oi} is the Förster distance of Alexa Fluor 350 and IAF, and $\rho(R)$ is the distance distribution function, assumed to be sum of Gaussi-

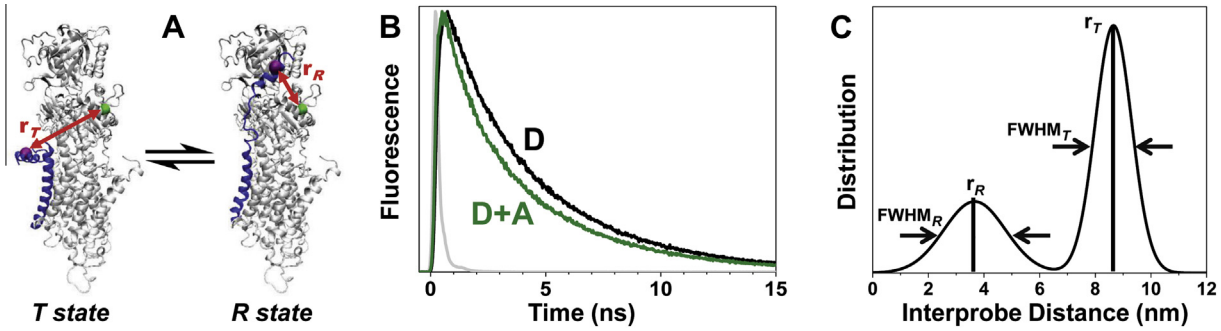

Fig. 1. TR-FRET experimental design. (A) Models of SERCA–PLB complex. SERCA (silver)–bound PLB (blue) is proposed to exist in an equilibrium between *T* and *R* states, as shown previously by EPR [24]. There is no high-resolution structure of the SERCA–PLB complex, but a model for the *R* state (right) is from [36], and the *T* state model (left) is based on the NMR structure of PLB. The labeling sites on SERCA (C674) and PLB (Y6C) are shown as green and magenta spheres, respectively. The interprobe distances in *T* and *R* states are denoted as r_T and r_R, respectively. Image created in VMD [45]. (B) Representative fluorescence waveforms. D, donor only. D + A, donor plus acceptor. Grey indicates instrument response function. (C) Interprobe distance distributions resolved from fluorescence waveforms in (B). Two Gaussian distance distributions were resolved. The shorter and longer distances correspond to *R* and *T* states, respectively [25].

ans, each with a mole fraction x_j, a center r_j and a full width at half maximum ($FWHM_j$) (Fig. 1C):

$$\rho(R) = \sum_{j=1}^{2} x_j \left(\frac{1}{\sigma_j\sqrt{2\pi}}\right) \exp\left[-\frac{(R-r_j)^2}{2\sigma_j^2}\right] \quad (5)$$

$$\text{where } \sigma_j = \frac{FWHM_j}{2\sqrt{2\ln 2}}$$

We assumed that PLB and pPLB populate the same two states, because the distance parameters resolved from independent fittings are similar for PLB and pPLB (Fig. S2) and this assumption does not change the goodness of the fit (Fig. S3). Our previous FRET studies showed that the shorter distance observed between probes on the SERCA and PLB cytoplasmic domains is the *R* state (correlating with decreased inhibition), while the longer distance is due to the *T* state, in which the PLB cytoplasmic domain interacts with membrane surface and hence increases interprobe distance [25]. Therefore, we refer the parameters of the shorter distance with a subscript *R*, and those of the longer distance with a subscript *T* (Fig. 1).

2.6. Statistical analysis

Data is presented as the mean ± SE. For comparison between two groups, a student's *t*-test was performed. A *p*-value less than 0.05 was taken as significant.

3. Results

3.1. Function of labeled SERCA and PLB

To confirm that the labeled proteins preserve their functions, we co-reconstituted SERCA and PLB into lipid vesicles and measured the Ca^{2+}-dependent ATPase activity. The function of unlabeled PLB is characterized by inhibition of SERCA (decreasing pK_{Ca}) and reversal after phosphorylation at S16 by PKA (Fig. 2). For unlabeled SERCA, pK_{Ca} = 6.43 ± 0.02, unlabeled PLB shifted pK_{Ca} to 6.32 ± 0.003, and unlabeled pPLB restored pK_{Ca} to 6.39 ± 0.02. Labeled proteins demonstrated similar results (Fig. 2). The pK_{Ca} of acceptor-labeled SERCA is 6.45 ± 0.02, donor-labeled PLB shifted it to 6.32 ± 0.003, and phosphorylated donor-labeled PLB shifted it back to 6.45 ± 0.01. Therefore, the fluorophore-labeled SERCA and PLB retained their functions, and these samples should provide reliable information of the conformational rearrangement induced by phosphorylation of S16 by PKA.

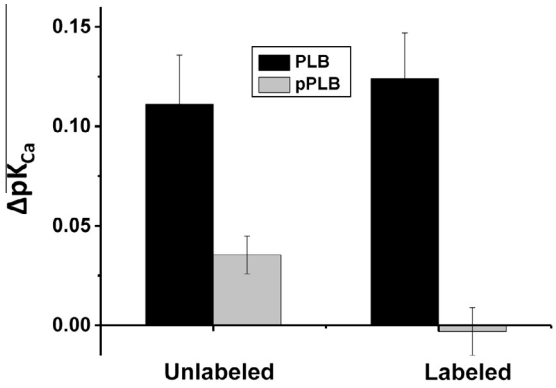

Fig. 2. Functional effect of PLB phosphorylation (as measured by ΔpK_{Ca}) is not affected by FRET labeling of SERCA and PLB. The molar ratio of Lipid:PLB:SERCA is 700:5:1. $n \geqslant 3$.

3.2. TR-FRET within the SERCA–PLB complex

Time-resolved fluorescence of donor-labeled PLB was measured in the presence of either unlabeled or acceptor-labeled SERCA with a PLB to SERCA molar ratio of 0.2. The fluorescence waveforms were then fitted by the equations described in Materials and Methods. TR-FRET data was fitted to two Gaussian distance distributions [25], assuming that PLB and pPLB populate the same two structural states (Figs. S2 and S3). At pCa 8.0, the shorter distance, r_R, is 3.52 ± 0.42 nm and the longer distance, r_T, is 8.27 ± 0.27 nm (Fig. 3A and B). The distance between the labeling sites predicted by the SERCA–PLB model is 2.69 nm (Fig. 1A, right) [36]. Crosslinking showed previously that K3 of PLB was within 1.5 nm of SERCA K400 [11]. The distance between C674 and K400 predicted by a crystal structure in the absence of Ca is 3.48 nm (3B9R) [37], consistent with our measurement for r_R. The fraction of pPLB that binds to SERCA (x_{DA}) decreased significantly from that of PLB, from 0.99 ± 0.01 to 0.50 ± 0.06 (Fig. 3C), indicating that the SERCA–PLB complex partially dissociates after PLB phosphorylation. Within the bound population, the fraction of the *R* state, x_R, is substantially increased after PLB phosphorylation, from 0.33 ± 0.04 to 0.68 ± 0.04 (Fig. 3A and D), indicating a substantial shift of the *T*/*R* equilibrium toward the *R* state.

Interprobe distances were measured at three Ca^{2+} concentrations, and no significant effects of Ca^{2+} were observed in binding or structure (Fig. 3 and Table S1). These results show clearly that PLB remains bound to SERCA after the E2 (Ca-free) to E1 (Ca-

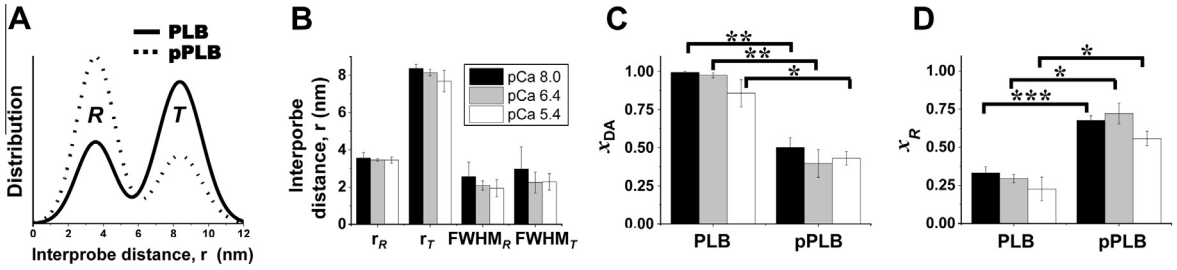

Fig. 3. TR-FRET shows that phosphorylation of PLB partially dissociates the SERCA–PLB complex and shifts the population to the shorter distance distribution. (A) Two Gaussian distance distributions (two structural states of SERCA–PLB, *R* and *T*) were needed to fit the TR-FRET data. (B) Centers (r) and widths (FWHM) of distance distributions. (C) Compared to PLB, phosphorylated PLB decreased the mole fraction of SERCA-bound PLB (x_{DA}), but did not abolish it. (D) The mole fraction of the short distance component (x_R) increased after phosphorylation. SERCA: PLB = 5. Lipid: SERCA = 200. $n \geqslant 3$. $^{*}p < 0.05$, $^{**}p < 0.01$, $^{***}p < 0.001$.

bound) transition. This result is consistent with previous FRET findings that the SERCA–PLB complex does not dissociate at physiological Ca^{2+} concentrations [17,19].

4. Discussion

We have performed TR-FRET on fluorophore-labeled SERCA and PLB co-reconstituted into lipid vesicles, to probe the structural mechanism for relief of inhibition by PLB phosphorylation and by micromolar Ca^{2+}. The functions of the proteins were preserved after covalent modification with fluorophores (Fig. 2). TR-FRET analysis showed that phosphorylation of PLB partially dissociates the SERCA–PLB complex and shifts the SERCA-bound PLB toward the less inhibitory *R* state. Ca^{2+} does not dissociate the complex or perturb the *T*-*R* equilibrium (Fig. 3).

The mechanism of relief of inhibition due to PLB phosphorylation has been controversial. Phosphorylation of PLB has been found to perturb the physical interaction between SERCA and PLB, as detected by decreases in crosslinking [14] and co-immunoprecipitation [15]. One study in living cells, using fluorescent fusion proteins, reported that phosphomimetic PLB mutations decreased FRET between SERCA and PLB [38], while another study reported increased FRET upon PLB phosphorylation [20]. Due to the steady-state nature of these FRET measurements, it is not clear whether changes in FRET were due to changes in SERCA–PLB association or to changes in the donor–acceptor distance within the complex. In the present study, this ambiguity was removed by the detection of time-resolved fluorescence, which simultaneously and independently resolves changes in binding and structure [25]. TR-FRET showed that 40–50% of PLB remains bound to SERCA after phosphorylation (Fig. 3C), even though phosphorylation completely relieves SERCA inhibition (Fig. 2). Therefore, the activity of the SERCA–pPLB complex is comparable to that of SERCA alone, and the relief of inhibition in the bound complex must be due to a structural change within the SERCA–pPLB complex.

To assess the physiological significance of the two observed effects – dissociation and structural change, it is important to compare the composition of our reconstituted samples with those in cardiac SR. In the present study with a fluorescent donor on PLB, acceptor-labeled SERCA was in 5-fold excess over PLB, to maximize the precision of FRET measurements. However, in cardiac SR, as in our functional measurements (Fig. 2), PLB is in large excess (3–5-fold) over SERCA [39]. Based on the affinity of SERCA for pPLB indicated from Fig. 3, and on the known concentrations of SERCA and PLB in cardiac SR [39,40], 76 ± 2% of SERCA in cardiac SR contains bound pPLB, even after complete phosphorylation of PLB (Table S2). This is consistent with EPR and NMR findings that pPLB remains bound to SERCA [18,23], with allosteric relief of inhibition achieved by shifting the *T*/*R* equilibrium toward the *R* state [23,24].

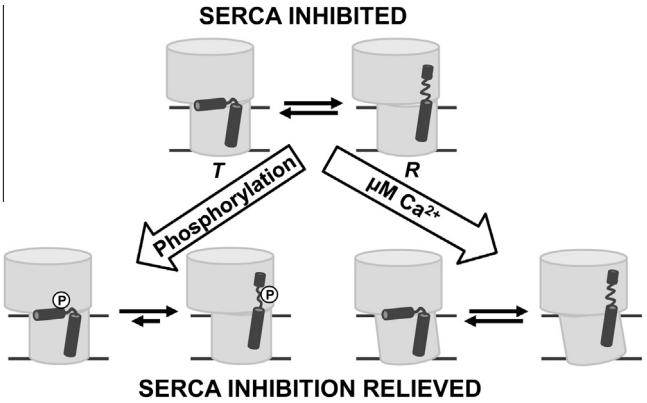

Fig. 4. Two mechanisms to relieve SERCA inhibition by PLB in cardiac SR. Phosphorylation shifts the PLB cytoplasmic domain toward the dynamically disordered *R* state. Micromolar Ca^{2+} induces a structural change in the SERCA transmembrane domain.

The present study clearly supports this "subunit" model for SERCA regulation (Fig. 4, left) over the dissociation model.

Although both dissociation and subunit models have been proposed to explain the mechanism of relief of inhibition by micromolar Ca^{2+} [12,13,16,17,19], our TR-FRET data showed no Ca-dependent changes in either binding or structure (Fig. 3B–D), clearly ruling out the dissociation model, but also showing clearly that Ca^{2+} relieves SERCA–PLB inhibition by a different mechanism from that of phosphorylation. This result is consistent with previous steady-state FRET studies showing little or no dissociation of PLB from SERCA due to Ca^{2+} [17,19]. Ca^{2+} is known to induce structural changes in its activation of SERCA [41,42], but these changes apparently do not perturb the distance between our labeling sites in the cytoplasmic domains of SERCA and PLB. This conclusion is consistent with structural models, since the distance between SERCA C674 (our acceptor labeling site) and K400 (proposed to lie in the binding groove of the PLB cytoplasmic domain, where our donor is located), changes only from 3.48 nm in the Ca-free crystal structure to 3.41 nm in the Ca-bound structure [37,43]. Since SERCA inhibition by PLB is caused by interaction of the transmembrane domains of the two proteins [44], we propose that Ca-induced structural changes in the SERCA transmembrane domain disrupt this inhibitory interaction, without changing interactions of the cytoplasmic domains, and without producing a substantial decrease in SERCA–PLB affinity (Fig. 4, right). This rearrangement of transmembrane helices would explain the Ca-induced decrease in crosslinking between the transmembrane domains of SERCA and PLB [12,13,16].

In summary, we conclude that phosphorylation of PLB and Ca^{2+} relieve SERCA inhibition through different mechanisms (Fig. 4), neither of which relies primarily on dissociation of the SERCA–PLB complex. PLB phosphorylation acts by promoting the dynamic disorder of the PLB cytoplasmic domain, while Ca^{2+} acts by changing the structure of the transmembrane domain of SERCA. Both mechanisms must disrupt the inhibitory interactions between the two transmembrane domains, by distinct mechanisms that remain to be elucidated (Fig. 4).

Acknowledgments

We thank Razvan Cornea and Elizabeth Lockamy for helpful discussions, Zachary James for help with mutagenesis and PLB expression, Ji Li and Kurt C. Peterson for technical support. Work was supported by grants NIH GM27906 and NIH AR0507220 to D.D.T.

Appendix A. Supplementary data

Supplementary data associated with this article can be found, in the online version, at http://dx.doi.org/10.1016/j.bbrc.2014.04.166.

References

[1] J.K. Gwathmey, L. Copelas, R. MacKinnon, F.J. Schoen, M.D. Feldman, W. Grossman, J.P. Morgan, Abnormal intracellular calcium handling in myocardium from patients with end-stage heart failure, Circ. Res. 61 (1987) 70–76.
[2] D.M. Bers, S. Despa, Cardiac myocytes Ca2+ and Na+ regulation in normal and failing hearts, J. Pharmacol. Sci. 100 (2006) 315–322.
[3] G. Inesi, F. Tadini-Buoninsegni, Ca^{2+}/H^{+} exchange, lumenal Ca^{2+} release and Ca^{2+}/ATP coupling ratios in the sarcoplasmic reticulum ATPase, J. Cell Commun. Signal. 8 (2014) 5–11.
[4] T. Cantilina, Y. Sagara, G. Inesi, L.R. Jones, Comparative studies of cardiac and skeletal sarcoplasmic reticulum ATPases. Effect of a phospholamban antibody on enzyme activation by Ca2+, J. Biol. Chem. 268 (1993) 17018–17025.
[5] A. Mattiazzi, C. Mundina-Weilenmann, C. Guoxiang, L. Vittone, E. Kranias, Role of phospholamban phosphorylation on Thr17 in cardiac physiological and pathological conditions, Cardiovasc. Res. 68 (2005) 366–375.
[6] J.K. Gwathmey, A. Yerevanian, R.J. Hajjar, Targeting sarcoplasmic reticulum calcium ATPase by gene therapy, Hum. Gene Ther. 24 (2013) 937–947.
[7] S. Minamisawa, M. Hoshijima, G. Chu, C.A. Ward, K. Frank, Y. Gu, M.E. Martone, Y. Wang, J. Ross Jr., E.G. Kranias, W.R. Giles, K.R. Chien, Chronic phospholamban-sarcoplasmic reticulum calcium ATPase interaction is the critical calcium cycling defect in dilated cardiomyopathy, Cell 99 (1999) 313–322.
[8] M. Hoshijima, Y. Ikeda, Y. Iwanaga, S. Minamisawa, M.O. Date, Y. Gu, M. Iwatate, M. Li, L. Wang, J.M. Wilson, Y. Wang, J. Ross Jr., K.R. Chien, Chronic suppression of heart-failure progression by a pseudophosphorylated mutant of phospholamban via in vivo cardiac rAAV gene delivery, Nat. Med. 8 (2002) 864–871.
[9] Y. Iwanaga, M. Hoshijima, Y. Gu, M. Iwatate, T. Dieterle, Y. Ikeda, M.O. Date, J. Chrast, M. Matsuzaki, K.L. Peterson, K.R. Chien, J. Ross Jr., Chronic phospholamban inhibition prevents progressive cardiac dysfunction and pathological remodeling after infarction in rats, J. Clin. Invest. 113 (2004) 727–736.
[10] M. Jessup, B. Greenberg, D. Mancini, T. Cappola, D.F. Pauly, B. Jaski, A. Yaroshinsky, K.M. Zsebo, H. Dittrich, R.J. Hajjar, Calcium upregulation by percutaneous administration of gene therapy in cardiac disease (CUPID): a phase 2 trial of intracoronary gene therapy of sarcoplasmic reticulum Ca2+-ATPase in patients with advanced heart failure, Circulation 124 (2011) 34–313.
[11] P. James, M. Inui, M. Tada, M. Chiesi, E. Carafoli, Nature and site of phospholamban regulation of the Ca2+ pump of sarcoplasmic reticulum, Nature 342 (1989) 90–92.
[12] Z. Chen, B.L. Akin, L.R. Jones, Ca2+ binding to site I of the cardiac Ca2+ pump is sufficient to dissociate phospholamban, J. Biol. Chem. 285 (2010) 3253–3260.
[13] Z. Chen, D.L. Stokes, W.J. Rice, L.R. Jones, Spatial and dynamic interactions between phospholamban and the canine cardiac Ca2+ pump revealed with use of heterobifunctional cross-linking agents, J. Biol. Chem. 278 (2003) 48348–48356.
[14] T. Morita, D. Hussain, M. Asahi, T. Tsuda, K. Kurzydlowski, C. Toyoshima, D.H. Maclennan, Interaction sites among phospholamban, sarcolipin, and the sarco(endo)plasmic reticulum Ca(2+)-ATPase, Biochem. Biophys. Res. Commun. 369 (2008) 188–194.
[15] M. Asahi, E. McKenna, K. Kurzydlowski, M. Tada, D.H. MacLennan, Physical interactions between phospholamban and sarco(endo)plasmic reticulum Ca2+-ATPases are dissociated by elevated Ca2+, but not by phospholamban phosphorylation, vanadate, or thapsigargin, and are enhanced by ATP, J. Biol. Chem. 275 (2000) 15034–15038.
[16] N.C. Bal, S.K. Maurya, D.H. Sopariwala, S.K. Sahoo, S.C. Gupta, S.A. Shaikh, M. Pant, L.A. Rowland, E. Bombardier, S.A. Goonasekera, A.R. Tupling, J.D. Molkentin, M. Periasamy, Sarcolipin is a newly identified regulator of muscle-based thermogenesis in mammals, Nat. Med. 18 (2012) 1575–1579.
[17] B. Mueller, C.B. Karim, I.V. Negrashov, H. Kutchai, D.D. Thomas, Direct detection of phospholamban and sarcoplasmic reticulum Ca-ATPase interaction in membranes using fluorescence resonance energy transfer, Biochemistry 43 (2004) 8754–8765.
[18] Z.M. James, J.E. McCaffrey, K.D. Torgersen, C.B. Karim, D.D. Thomas, Protein–protein interactions in calcium transport regulation probed by saturation transfer electron paramagnetic resonance, Biophys. J. 103 (2012) 1370–1378.
[19] P. Bidwell, D.J. Blackwell, Z. Hou, A.V. Zima, S.L. Robia, Phospholamban binds with differential affinity to calcium pump conformers, J. Biol. Chem. 286 (2011) 35044–35050.
[20] S.J. Gruber, S. Haydon, D.D. Thomas, Phospholamban mutants compete with wild type for SERCA binding in living cells, Biochem. Biophys. Res. Commun. 420 (2012) 236–240.
[21] C.B. Karim, T.L. Kirby, Z. Zhang, Y. Nesmelov, D.D. Thomas, Phospholamban structural dynamics in lipid bilayers probed by a spin label rigidly coupled to the peptide backbone, Proc. Natl. Acad. Sci. U.S.A. 101 (2004) 14437–14442.
[22] Y.E. Nesmelov, C.B. Karim, L. Song, P.G. Fajer, D.D. Thomas, Rotational dynamics of phospholamban determined by multifrequency electron paramagnetic resonance, Biophys. J. 93 (2007) 2805–2812.
[23] M. Gustavsson, R. Verardi, D.G. Mullen, K.R. Mote, N.J. Traaseth, T. Gopinath, G. Veglia, Allosteric regulation of SERCA by phosphorylation-mediated conformational shift of phospholamban, Proc. Natl. Acad. Sci. U.S.A. 110 (2013) 17338–17343.
[24] C.B. Karim, Z. Zhang, E.C. Howard, K.D. Torgersen, D.D. Thomas, Phosphorylation-dependent conformational switch in spin-labeled phospholamban bound to SERCA, J. Mol. Biol. 358 (2006) 1032–1040.
[25] J. Li, Z.M. James, X. Dong, C.B. Karim, D.D. Thomas, Structural and functional dynamics of an integral membrane protein complex modulated by lipid headgroup charge, J. Mol. Biol. 418 (2012) 379–389.
[26] J.L. Fernandez, M. Rosemblatt, C. Hidalgo, Highly purified sarcoplasmic reticulum vesicles are devoid of Ca2+- independent ('basal') ATPase activity, Biochim. Biophys. Acta 599 (1980) 552–568.
[27] D.L. Stokes, N.M. Green, Three-dimensional crystals of CaATPase from sarcoplasmic reticulum. Symmetry and molecular packing, Biophys. J. 57 (1990) 1–14.
[28] J.E. Bishop, T.C. Squier, D.J. Bigelow, G. Inesi, (Iodoacetamido)fluorescein labels a pair of proximal cysteines on the Ca2+-ATPase of sarcoplasmic reticulum, Biochemistry 27 (1988) 5233–5240.
[29] R.L. Cornea, L.R. Jones, J.M. Autry, D.D. Thomas, Mutation and phosphorylation change the oligomeric structure of phospholamban in lipid bilayers, Biochemistry 36 (1997) 2960–2967.
[30] A. Mascioni, C. Karim, J. Zamoon, D.D. Thomas, G. Veglia, Solid-state NMR and rigid body molecular dynamics to determine domain orientations of monomeric phospholamban, J. Am. Chem. Soc. 124 (2002) 9392–9393.
[31] J. Zamoon, F. Nitu, C. Karim, D.D. Thomas, G. Veglia, Mapping the interaction surface of a membrane protein: unveiling the conformational switch of phospholamban in calcium pump regulation, Proc. Natl. Acad. Sci. U.S.A. 102 (2005) 4747–4752.
[32] B. Buck, J. Zamoon, T.L. Kirby, T.M. DeSilva, C. Karim, D. Thomas, G. Veglia, Overexpression, purification, and characterization of recombinant Ca-ATPase regulators for high-resolution solution and solid-state NMR studies, Protein Expr. Purif. 30 (2003) 253–261.
[33] L.G. Reddy, R.L. Cornea, D.L. Winters, E. McKenna, D.D. Thomas, Defining the molecular components of calcium transport regulation in a reconstituted membrane system, Biochemistry 42 (2003) 4585–4592.
[34] E.L. Lockamy, R.L. Cornea, C.B. Karim, D.D. Thomas, Functional and physical competition between phospholamban and its mutants provides insight into the molecular mechanism of gene therapy for heart failure, Biochem. Biophys. Res. Commun. 408 (2011) 388–392.
[35] J.R. Lakowicz, Principles of Fluorescence Spectroscopy, third ed., Springer Science + Business Media, LLC, New York, 2006.
[36] C. Toyoshima, M. Asahi, Y. Sugita, R. Khanna, T. Tsuda, D.H. MacLennan, Modeling of the inhibitory interaction of phospholamban with the Ca2+ ATPase, Proc. Natl. Acad. Sci. U.S.A. 100 (2003) 467–472.
[37] C. Olesen, M. Picard, A.M. Winther, C. Gyrup, J.P. Morth, C. Oxvig, J.V. Moller, P. Nissen, The structural basis of calcium transport by the calcium pump, Nature 450 (2007) 1036–1042.
[38] Z. Hou, E.M. Kelly, S.L. Robia, Phosphomimetic mutations increase phospholamban oligomerization and alter the structure of its regulatory complex, J. Biol. Chem. 283 (2008) 28996–29003.
[39] D.A. Ferrington, Q. Yao, T.C. Squier, D.J. Bigelow, Comparable levels of Ca-ATPase inhibition by phospholamban in slow-twitch skeletal and cardiac sarcoplasmic reticulum, Biochemistry 41 (2002) 13289–13296.
[40] R.W. Gross, Identification of plasmalogen as the major phospholipid constituent of cardiac sarcoplasmic reticulum, Biochemistry 24 (1985) 1662–1668.
[41] L.M. Espinoza-Fonseca, D.D. Thomas, Atomic-level characterization of the activation mechanism of SERCA by calcium, PLoS One 6 (2011) e26936.

[42] Z. Hou, S. Hu, D.J. Blackwell, T.D. Miller, D.D. Thomas, S.L. Robia, Two-color calcium pump reveals closure of the cytoplasmic headpiece with calcium binding, PLoS One 7 (2012) e40369.
[43] A.M. Jensen, T.L. Sorensen, C. Olesen, J.V. Moller, P. Nissen, Modulatory and catalytic modes of ATP binding by the calcium pump, EMBO J. 25 (2006) 2305–2314.
[44] C.B. Karim, C.G. Marquardt, J.D. Stamm, G. Barany, D.D. Thomas, Synthetic null-cysteine phospholamban analogue and the corresponding transmembrane domain inhibit the Ca-ATPase, Biochemistry 39 (2000) 10892–10897.
[45] W. Humphrey, A. Dalke, K. Schulten, VMD: visual molecular dynamics, J. Mol. Graph. 14 (33–38) (1996) 27–38.